

Magnetization dependence on strain in the Ni–Mn–Ga magnetic shape memory material

I. Suorsa, E. Pagounis,^{a)} and K. Ullakko
AdaptaMat Ltd, Yrityspiha 5, 00390 Helsinki, Finland

(Received 12 January 2004; accepted 13 April 2004; published online 19 May 2004)

Magnetic shape memory (MSM) materials can generate up to 10% strain when exposed to a magnetic field. The magnetization of the MSM material is closely related to its strain level. Modeling this relationship is of prime importance, especially in sensor and motion generation applications. In the present work, the magnetization curve of a Ni₂MnGa MSM material was measured at different strain levels. The measurements were performed at magnetic fields of up to 130 kA/m, which includes the range used in most sensor applications. The measurement setup is described, and the results are compared with two models of magnetization dependence on strain, a linear and a nonlinear model. It is demonstrated that at high magnetic field strength values the relationship is linear, while at low fields ($H < 40$ kA/m) the dependence between the strain and the magnetization is nonlinear. © 2004 American Institute of Physics. [DOI: 10.1063/1.1759771]

Magnetic shape memory (MSM) materials generate stress and change their shape in the magnetic field.^{1–4} The deformation of these materials can be as large as 10%, depending on their structure and chemical composition.¹ Therefore, the material has significant potential in motion generation applications, such as actuators.⁵ In addition, the reverse MSM effect can be used for position, speed, or acceleration sensors, as well as voltage generators.^{6,7} Several models of the MSM effect have been proposed.^{8–10} The dependence of the magnetization on the MSM material's strain is of prime importance.⁹ However, no comprehensive measurement results have been reported so far.¹¹ The aim of the present study is to measure the magnetization curve of the MSM material as a function of the strain at low magnetic field strengths ($H < 130$ kA/m). These fields include those utilized in most sensor and voltage generation applications, while they also provide a strong indication of the magnetization-strain relationship in higher magnetic fields.

The MSM material consists of twin variants, which are magnetically anisotropic (Fig. 1). For modeling purposes we assume the MSM material as a homogeneous object. Accordingly, we use average values of the magnetic field inside the MSM material to describe the magnetic state of it. It has been proposed that the average, or effective, magnetization of the MSM material is linearly dependent on the variant proportion x .¹⁰ This variant proportion can be written, as a function of strain ε , as $x = \varepsilon/\varepsilon_{\max}$, where ε_{\max} is the maximum magnetic field induced strain. According to the linear assumption the effective flux density of the MSM material is

$$B(H, \varepsilon) = B_t(H) + \frac{\varepsilon}{\varepsilon_{\max}} [B_a(H) - B_t(H)], \quad (1)$$

where $B_t(H)$ is the flux density along the hard magnetization direction, $B_a(H)$ is the flux density along the easy magnetization direction, and H is the magnetic field strength. In this

case the field strength is assumed constant along the MSM material. The above dependence assumes that the variants in the material are magnetically parallel. The other extreme is when the variants are considered to be in series. In this case the flux density is constant through the MSM material, and, by using Ampere's law, the average field strength depends on the strain according to the relation

$$H(B, \varepsilon) = H_t(B) + \frac{\varepsilon}{\varepsilon_{\max}} [H_a(B) - H_t(B)], \quad (2)$$

where $H_a(B)$ is the magnetic field strength along the easy magnetization direction, and $H_t(B)$ is the magnetic field strength along the hard magnetization direction. In case the permeabilities of the hard axis and the easy axis of magnetization are constant then, at constant field strength values, from Eq. (2) it follows that the effective flux density in the MSM material is

$$B(H, \varepsilon) = \frac{B_t(H)B_a(H)}{B_t(H) + \frac{\varepsilon}{\varepsilon_{\max}} [B_a(H) - B_t(H)]}. \quad (3)$$

Magnetization measurements were performed with the setup presented in Fig. 2. A nonstoichiometric Ni₂MnGa MSM material with the dimensions of 5.15×5.0×19.35 mm³ was used for the measurements. The sample was cut along the (100) direction, mechanically polished, and finally electropolished. After this initial treatment the sample was tightly placed between ferromagnetic plates, which in turn were placed in the air-gap of a large electromagnet. The electromagnet's bore diameter was 40 mm. The flux density and the field strength in the MSM material were derived from the induced voltages of two types of measurement coils, as shown in Fig. 2. The flux density measurement coil was placed around the material, while the field strength measurement coils were placed next to the material. Because the coils cover the whole air-gap length they can sense the average field values in the MSM material. The field strength was calculated by intergrading the induced voltage from the field

^{a)}Author to whom correspondence should be addressed; electronic mail: pagounis@adaptamat.com

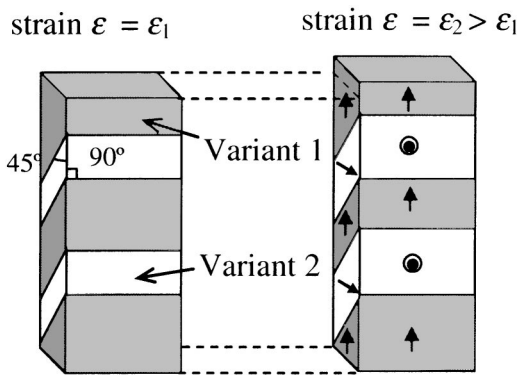


FIG. 1. A schematic representation of the twin variant structure of the MSM material at two strain states. The variant with a preferred orientation relative to the magnetic field, or to mechanical stress, grows at the expense of the other variant. The arrows indicate the direction of the magnetic domain walls and of the magnetization.

strength measurement coils. The flux density coil also enclosed a large cross-section area of air. Therefore, the flux density in the MSM material was calculated by intergrading the induced voltage from the coil and subtracting the flux of the air cross section from the results. The measurement accuracy of the coils was verified with a Hall sensor (accuracy 1%), placed in the air gap with the coils.

The electromagnet was run with a low frequency alternating current (4 Hz) to minimize the effect of the eddy currents. The induced voltages were measured with a HP 54603 digital oscilloscope. The magnetization curves at different strain values are summarized in Fig. 3. The results demonstrate that when the strain increases the MSM material permeability decreases, and the “knee” of the magnetization curve moves towards higher field strength values. Extrapolation of the magnetization curves gives the crossing point of the curves at about 500 kA/m, which is in accordance with earlier measurements in Ni–Mn–Ga alloys.^{3,11}

The measured flux density inside the MSM material as a function of the material’s strain is presented in Fig. 4. It is seen that the relationship between the flux density and the MSM material strain is mainly linear, which is in accordance with previous modeling work.^{9,10} On the other hand, at low

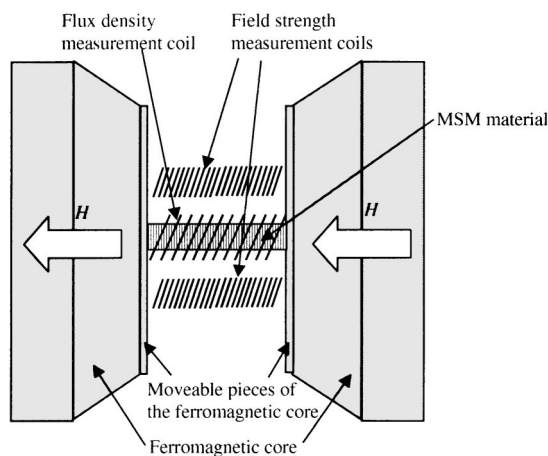


FIG. 2. Magnetization measurement setup. The field strength measurement coils have 807 turns and the flux density measurement coil has 271 turns. The magnetization was measured along the long dimension of the MSM material.

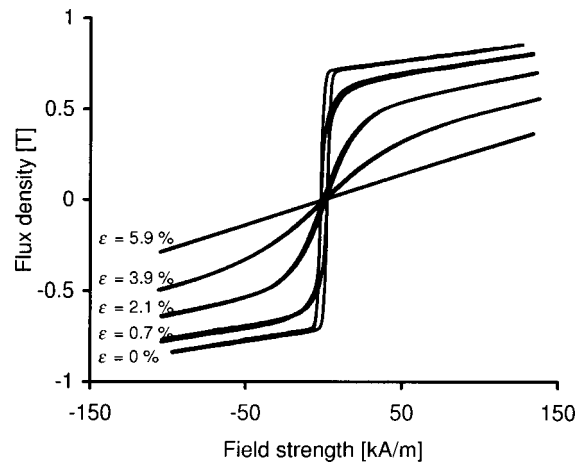


FIG. 3. Magnetization curves of the MSM material at different strain levels.

fields (5 kA/m) the dependence is clearly nonlinear. In Fig. 4 the calculated, using Eq. (1), results are also presented with the straight lines. In the case of field value of 5 kA/m, both the linear [Eq. (1)] and the nonlinear [Eq. (3)] calculated results are presented. It is seen that at low fields, neither of the calculated results can accurately model the measured ones and the measured curve is between the two model results. At high magnetic fields the strain dependence becomes more and more linear, up to 130 kA/m, and the results indicate that similar behavior is also expected at higher magnetic fields.

In Fig. 5 an optical micrograph of the MSM material after the testing is presented. Sample is at 1.8% strain, which explains the residual twin structure shown in the Fig. 5. It is seen that the twin areas vary in size, while there is an angle between the twin boundary and the side of the sample. The angle measured is 3°, which represents the deviation from a perfect orientation, shown in Fig. 1. The orientation angle variation does not, however, significantly affect the measurement results.

As a summary, the magnetization curve of the Ni₂MnGa MSM material was measured at different strain values. The

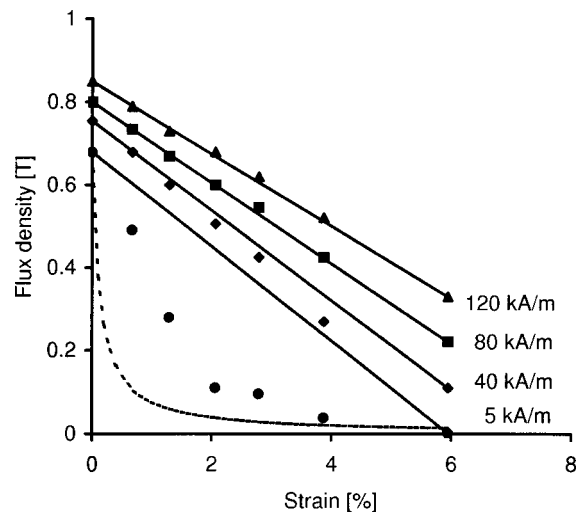


FIG. 4. The flux density in the MSM material as a function of the strain. The calculated, with linear model, results are presented with the straight lines. For the 5 kA/m field the nonlinear model results are also shown with the dashed line.



FIG. 5. Optical micrograph of the twin boundary structure of the studied MSM material at 1.8% strain. The two variants can be seen as dark and light areas on the surface.

results demonstrate a clear dependence of the magnetization and the flux density on the strain level of the MSM material, which is in accordance with previous theory. It was found that at magnetic field strength values of larger than 40 kA/m the dependence is linear, according to Eq. (1). At lower field values the linear assumption becomes less accurate. Because

in actuator applications the magnetic fields are relatively high, the linear approximation can be used in their design. On the other hand, linear approximation is not valid for the sensor applications, where the magnetic fields are usually low. The nonlinear region is connected to the field strength value of the knee of the magnetization curve, which depends on strain. At higher magnetic field strength values the dependence between the strain and the flux density in the MSM material becomes linear.

¹A. Sozinov, A. A. Likhachev, N. Lanska, and K. Ullakko, *Appl. Phys. Lett.* **80**, 1746 (2002).

²K. Ullakko, J. K. Huang, C. Kantner, and R. C. O'Handley, *Appl. Phys. Lett.* **69**, 1966 (1996).

³S. J. Murray, M. Marioni, S. M. Allen, and R. C. O'Handley, *Appl. Phys. Lett.* **77**, 886 (2000).

⁴M. Wuttig, L. Liu, K. Tsuchiya, and R. D. James, *J. Appl. Phys.* **87**, 4707 (2000).

⁵J. Tellinen, I. Suorsa, A. Jääskeläinen, I. Aaltio, and K. Ullakko, *Proceedings ACTUATOR 2002, Eighth International Conference on New Actuators*, Bremen, Germany, 10–12 June 2002, p. 566.

⁶I. Suorsa, J. Tellinen, E. Pagounis, I. Aaltio, and K. Ullakko, in *Ref. 5*, p. 158.

⁷P. Müllner, V. A. Chernenko, and G. Kostorz, *Scr. Mater.* **49**, 129 (2003).

⁸R. D. James and M. Wuttig, *Philos. Mag. A* **77**, 1273 (1998).

⁹A. Likhachev and K. Ullakko, *Eur. Phys. J. B* **14**, 263 (2000).

¹⁰R. C. O'Handley, *J. Appl. Phys.* **83**, 3263 (1998).

¹¹A. A. Likhachev, A. Sozinov, and K. Ullakko, *Proc. SPIE* **4699**, 553 (2002).